Acta Mechanica 63, 15—44 (1986)

ACTA MECHANICA

The Effects of an Impact Velocity Dependent Coefficient of Restitution on Stresses Developed by Sheared Granular Materials

By

C. K. K. Lun and **S. B. Savage**, Montreal, Québec

With 12 Figures

(*Received October 13, 1985; revised November 7, 1985*)

Summary

Following the granular flow kinetic theory of Lun, Savage, Jeffrey and Chepurniy, a moment method is used to obtain the approximate form for the single particle velocity distribution function for the case of smooth, slightly inelastic, uniform spherical particles in which the coefficient of restitution e depends upon the particle impact velocity. Constitutive equations for stress are derived and the theory is applied to the case of a simple shear flow. Theoretical predictions of stresses are compared with experimental results. The effect of the impact velocity dependent e is to cause the stresses to vary with the shear rate raised to a power less than two; this is consistent with the experimental observations. On the basis of the present theory and comparisons with experimental data it is concluded that theoretical models which include both surface friction and an impact velocity dependent e will lead to improved agreement between the theoretical predictions and the measurements.

1. Introduction

A number of recent studies dealing with the flow of granular materials considered the particle mechanics at the microstructural level. They incorporated the effects of material properties such as the coefficient of restitution, which are necessary to account for the dissipation of energy in inelastic grain interactions ([1]—[8]). All of the above work except the numerical simulation of Walton and Braun [8] has assumed a constant coefficient of restitution e for a specific granular material. However, from physical considerations, the results of theoretical analyses of the plastic deformations that occur during a collision, as well as from experimental evidence [9], it is apparent that e is dependent upon the impact velocity for a given granular material.

It is interesting to note that theoretical models using approaches analogous to the kinetic theory of dilute gases have been attempted in the context of astro-

physics and space science ([10]—[13]). Basically, these theories employed a modified integrodifferential Boltzmann equation of velocity distribution function for dilute gases which incorporated the effects of inelastic collisions between grains to study the formation of the Solar System and planetary rings such as Saturn's rings. Trulsen [10] and Hameen-Anttila [11] considered the case of a constant coefficient of restitution while Goldreich and Tremaine [12] assumed e to depend in a simple way upon the root mean square velocity of the particles.

In the present study, we extend the kinetic theory developed in Lun et al. [1] to the case where the coefficient of restitution of the granular materials depends upon the impact velocity during a binary collision between smooth, inelastic spherical particles. The case of simple shear will be studied in detail and the theoretical prediction of stresses will be compared with experimental measurements.

2. Kinetic Theory

The moment equation, the conservation equations of mass, momentum, translational kinetic fluctuation energy and the integral forms for the constitutive equations such as the rate of energy dissipation, stresses and kinetic fluctuation energy flux which were derived in [1], are still appropriate for the case of granular flows with materials having an impact velocity dependent coefficient of restitution e.

The ensemble average of the single-particle quantity ψ is defined as

$$\langle \psi \rangle = \frac{1}{n} \int \psi f^{(1)}(\boldsymbol{r}, \boldsymbol{c}; t)\, d\boldsymbol{c} \tag{1}$$

where n is the particle number density and $f^{(1)}$ is the single particle velocity distribution function. The equation of change for the mean value of particle quantity is

$$\frac{\partial}{\partial t} \langle n\psi \rangle = \langle D\psi \rangle - \nabla \cdot \langle n\boldsymbol{c}\psi \rangle + \nabla \cdot \boldsymbol{\theta} + \chi$$

and (2)

$$D\psi = \frac{\partial \psi}{\partial t} + \boldsymbol{c} \cdot \frac{\partial \psi}{\partial \boldsymbol{r}} + \frac{\boldsymbol{F}_0}{m} \cdot \frac{\partial \psi}{\partial \boldsymbol{c}}$$

where $\boldsymbol{c}$ is instantaneous particle velocity and $\boldsymbol{F}_0$ is the external force field. The collisional transfer contribution is

$$\boldsymbol{\theta} = -\frac{\sigma^3}{2} \int_{\boldsymbol{c}_{12} \cdot \boldsymbol{k} > 0} (\psi_1' - \psi_1)\, (\boldsymbol{c}_{12} \cdot \boldsymbol{k})\, \boldsymbol{k}\, f^{(2)}\left(\boldsymbol{r} - \tfrac{1}{2}\sigma\boldsymbol{k}, \boldsymbol{c}_1; \boldsymbol{r} + \tfrac{1}{2}\sigma\boldsymbol{k}, \boldsymbol{c}_2; t\right) \cdot d\boldsymbol{k}\, d\boldsymbol{c}_1\, d\boldsymbol{c}_2 \tag{3}$$

and the 'source-like' contribution is

$$\chi = \frac{\sigma^2}{2} \int_{\boldsymbol{c}_{12} \cdot \boldsymbol{k} > 0} (\psi_2' + \psi_1' - \psi_2 - \psi_1)\, (\boldsymbol{c}_{12} \cdot \boldsymbol{k})\, f^{(2)}(\boldsymbol{r} - \sigma\boldsymbol{k}, \boldsymbol{c}_1; \boldsymbol{r}, \boldsymbol{c}_2; t) \cdot d\boldsymbol{k}\, d\boldsymbol{c}_1\, d\boldsymbol{c}_2, \tag{4}$$

where subscripts 1 and 2 denote the quantities for particles 1 and 2 respectively.

By taking ψ to be m, $m\boldsymbol{c}$ and $mc^2/2$ in (2), we obtain the usual hydrodynamic equations

$$\frac{\partial \varrho}{dt} = -\varrho \nabla \cdot \boldsymbol{u} \tag{5}$$

$$\varrho \frac{d\boldsymbol{u}}{dt} = \varrho \boldsymbol{b} - \nabla \cdot \boldsymbol{P} \tag{6}$$

$$\frac{3}{2} \varrho \frac{dT}{dt} = -\boldsymbol{P} : \nabla \boldsymbol{u} - \nabla \cdot \boldsymbol{q} - \gamma. \tag{7}$$

In these equations $\varrho = mn = \nu \varrho_p$ is the bulk density, ν is the bulk solids fraction (volume of solids/total volume), ϱ_p is the mass density of an individual particle, $\boldsymbol{u} = \langle \boldsymbol{c} \rangle$ is the bulk velocity, $\boldsymbol{P}$ is the stress tensor and $\boldsymbol{b}$ is the body force per unit mass. Finally, $\frac{3}{2} T = \frac{1}{2} \langle C^2 \rangle$ is the specific kinetic energy of the velocity fluctuation energy where $\boldsymbol{C} = \boldsymbol{c} - \boldsymbol{u}$, and $\boldsymbol{q}$ is the flux of fluctuation energy. The quantity T is known as the granular 'temperature'.

The stress tensor $\boldsymbol{P}$ is the sum of a kinetic part $\boldsymbol{P}_k$ and a collisional part $\boldsymbol{P}_c$

$$\boldsymbol{P}_k = \varrho \langle \boldsymbol{CC} \rangle, \qquad \boldsymbol{P}_c = \boldsymbol{\theta}(m\boldsymbol{c}). \tag{8), (9}$$

Similarly, the flux of fluctuation energy $\boldsymbol{q}$ is the sum of a kinetic part $\boldsymbol{q}_k$ and a collisional part $\boldsymbol{q}_c$.

$$\boldsymbol{q}_k = \varrho \langle C^2 \boldsymbol{C} \rangle / 2, \qquad \boldsymbol{q}_c = \boldsymbol{\theta}(mC^2/2). \tag{10), (11}$$

The collisional rate of energy dissipation per unit volume is $\gamma = -\chi(mc^2/2)$.

3. Collision Model

Goldsmith [9] presented a number of experiments in which the coefficient of restitution for different materials was measured as a function of impact velocity. The values of e were found to decrease with increasing impact velocity. At very low impact velocity, where the particle deformation is essentially elastic and the energy dissipated is small, e has values close to one. At high impact velocity, where the effect of plastic deformation and energy dissipation are significant, e is small compared to unity. The case of zero e represents the situation where the colliding particles do not rebound after the collision.

A dimensional analysis for the collision between two identical inelastic spherical particles can be used to obtain an expression relating e to the relevant physical variables. The coefficient of restitution e may be expressed as follows

$$e = fn(\sigma, \varrho_p, |\boldsymbol{k} \cdot \boldsymbol{c}_{12}|, p_0, E, \nu_p, g), \tag{12}$$

where $\boldsymbol{c}_{12} = \boldsymbol{c}_1 - \boldsymbol{c}_2$ is the relative velocity and $\boldsymbol{k}$ is the unit vector between the centers of the two colliding particles, p_0 is the yield stress, E is the modulus of elasticity and ν_p is the Poisson's ratio and g is the gravitational acceleration. We may rewrite (12) in terms of dimensionless groups as follows

$$e = fn\left((\varrho_p/E)^{1/2} |\boldsymbol{k} \cdot \boldsymbol{c}_{12}|, p_0/E, \nu_p, p_0/(\varrho_p g \sigma)\right). \tag{13}$$

These non-dimensional groups, except the last one, are consistent with the theoretical analysis presented by Goldsmith [9] which accounted for the plastic deformation during the collision. If we multiply both the numerator and denominator of the last non-dimensional group in (13) by the square of the particle diameter, then it is clear that the group is proportional to the ratio of the force required to make the particle yield and its own weight. This non-dimensioal group is unlikely to be important for most practical granular materials. The analysis of Goldsmith [9] indicates that the coefficient of restitution is independent of the particle diameter for collisions between identical particles.

In the present analysis, the coefficient of restitution is *assumed* to decay exponentially with increasing impact velocity. This trend of reduction in e is

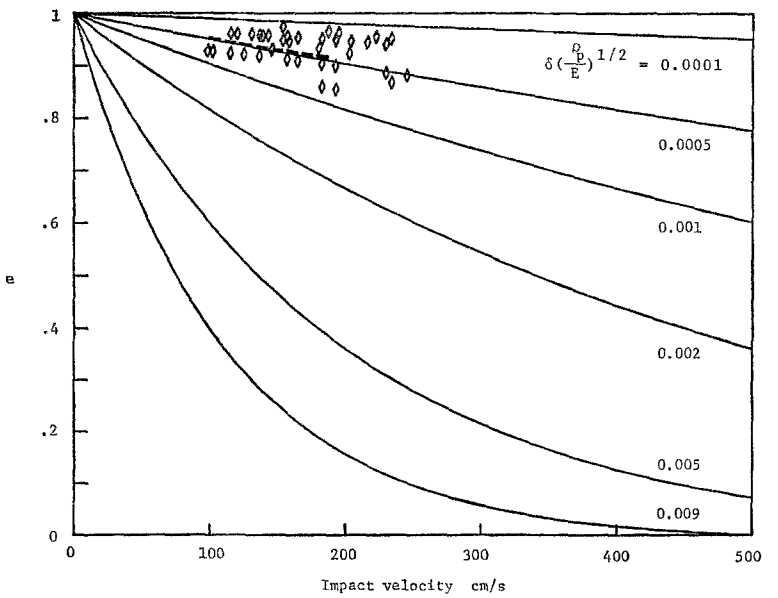

Fig. 1. Variation of coefficient of restitution e with impact velocity, ----, glass spheres [9]; ◇, present results for glass spheres

indicated by most of the experimental data obtained using different materials [9], i.e.

$$e = \exp\left[-\delta(\varrho_p/E)^{1/2}\,|\boldsymbol{k}\cdot\boldsymbol{c}_{12}|\right], \tag{14}$$

where δ is a non-dimensional coefficient. Moreover, an exponential decay function for the coefficient of restitution is very convenient for the computations of the constitutive integrals such as the stresses. Equation (14) is plotted in Fig. 1 as a function of $\delta(\varrho_p/E)^{1/2}$ and impact velocity. Laboratory experiments were performed to determine e versus impact velocity (see Appendix A for details) for glass spheres with diameters from 2.0 to 2.5 mm. The results of these experiments and those presented by Goldsmith yield a value for the group $\delta(\varrho_p/E)^{1/2}$ of about 0.0005 s/cm.

The derivations for the relationships between e, the precollisional and post-collisional velocities, and the translational energy lost during a collision were given in [1] and will not be repeated here.

4. Constitutive Equations

We follow the moment method used in [1] to obtain the single particle velocity distribution function and the constitutive relations. The calculations are much more involved and tedious than the previous case of a constant coefficient of restitution, hence we restrict our attention to the constitutive equations for the stresses which are sufficient to study the case of simple shear.

The singlet distribution function $f^{(1)}$ may be written in the form of a perturbation of the local Maxwellian distribution $f^{(0)}$

$$f^{(1)} = f^{(0)}\left(1 + a_1 \overset{0}{\boldsymbol{CC}} : \nabla\boldsymbol{u}\right), \tag{15}$$

where the traceless dyadic

$$\overset{0}{\boldsymbol{CC}} = \boldsymbol{CC} - \frac{1}{3}C^2\boldsymbol{I}. \tag{16}$$

We make the Enskog assumption for the pair velocity distribution function such that

$$f^{(2)}(\boldsymbol{r}_1, \boldsymbol{c}_1; \boldsymbol{r}_2, \boldsymbol{c}_2; t) = g_0(\nu)\, f^{(1)}(\boldsymbol{r} - \sigma\boldsymbol{k}, \boldsymbol{c}_1; t)\, f^{(1)}(\boldsymbol{r}, \boldsymbol{c}_2; t). \tag{17}$$

An empirical equation for the radial distribution function is employed (Appendix B)

$$g_0(\nu) = (1 - \nu/\nu_m)^{-5\nu_m/2}. \tag{18}$$

The coefficient a_1 may be determined using the moment method by considering the case of $\nabla\boldsymbol{u} = \boldsymbol{e}_x\boldsymbol{e}_y\, du/dy$ (where $\boldsymbol{u} = (u, v, w)$), T and n being constants and

taking moment of $\psi = c_x c_y$ in (2), (3) and (4). Thus we find

$$a_1 = -\frac{\mu}{\varrho T^2 g_0 b_1}\left(1 + \frac{8}{5} b_2 \nu g_0\right) \tag{19}$$

$$\mu = \frac{5m(T/\pi)^{1/2}}{16\sigma^2} \tag{20}$$

where μ is the shear viscosity for perfectly elastic particles (i.e. $\delta = 0$) at dilute concentration. By using (8) and (9), we may calculate the constitutive equation for the stresses. The kinetic and collisional contributions to the total stress tensor $\boldsymbol{P}$ are

$$\boldsymbol{P}_k = \varrho T \boldsymbol{I} - \frac{2\mu}{g_0 b_1}\left(1 + \frac{8}{5} b_2 \nu g_0\right) \boldsymbol{S} \tag{21}$$

$$\boldsymbol{P}_c = 4\varrho T b_6 \nu g_0 \boldsymbol{I} - \frac{16\mu\nu b_3}{5b_1}\left(1 + \frac{8}{5} b_2 \nu g_0\right) \boldsymbol{S} - \frac{256}{5\pi} b_4 \mu \nu^2 g_0 \left[\frac{6}{5}\boldsymbol{S} + (\nabla \cdot \boldsymbol{u})\,\boldsymbol{I}\right], \tag{22}$$

where

$$\boldsymbol{S} = \frac{1}{2}(u_{i,j} + u_{j,i}) - \frac{1}{3} u_{k,k}\delta_{ij}. \tag{23}$$

The total stress tensor may be written as

$$\begin{aligned} \boldsymbol{P} &= \boldsymbol{P}_k + \boldsymbol{P}_c \\ &= [\varrho T(1 + 4b_6 \nu g_0) - b_4 \mu_b \nabla \cdot \boldsymbol{u}]\,\boldsymbol{I} \\ &\quad - \left[\frac{2\mu}{b_1 g_0}\left(1 + \frac{8}{5} b_3 \nu g_0\right)\left(1 + \frac{8}{5} b_2 \nu g_0\right) + \frac{6}{5} b_4 \mu_b\right] \boldsymbol{S} \end{aligned} \tag{24}$$

where

$$\mu_b = \frac{256}{5\pi} \mu \nu^2 g_0 \tag{25}$$

is the bulk viscosity for perfectly elastic particles and $b_4 \mu_b$ is that property for the inelastic particles.

The expression for the collisional rate of energy dissipation per unit volume is

$$\gamma = \frac{12 \varrho_p \nu^2 g_0}{\pi^{1/2}\sigma} b_5 T^{3/2}. \tag{26}$$

The variables b_1 to b_6 are complicated functions of a nondimensional granular temperature T^* which is defined as

$$T^* = \delta^2(\varrho_p/E)\, T \tag{27}$$

and

$$b_1 = 1 - \frac{13}{6} T^* - \frac{8}{3} T^{*2} - \frac{(\pi T^*)^{1/2}}{3} (3 + 2T^{*2}) \exp(T^*) \operatorname{erfc}(T^{*1/2}) + (\pi T^*)^{1/2} \left(1 + 6T^* + \frac{16}{3} T^{*2}\right) \exp(4T^*) \operatorname{erfc}(2T^{*1/2}) \tag{28}$$

$$b_2 = -\frac{1}{4} - 2\left(\frac{T^*}{\pi}\right)^{1/2} (3 + 4T^*) + \left(\frac{1}{2} + T^*\right) \exp(T^*) \operatorname{erfc}(T^{*1/2}) + \left(\frac{3}{4} + 12T^* + 16T^{*2}\right) \exp(4T^*) \operatorname{erfc}(2T^{*1/2}) \tag{29}$$

$$b_3 = \frac{1}{2} + \frac{1}{2}(1 + 5T^* + 2T^{*2}) \exp(T^*) \operatorname{erfc}(T^{*1/2}) - \left(\frac{T^*}{\pi}\right)^{1/2} (2 + T^*) \tag{30}$$

$$b_4 = \frac{1}{2} + \frac{1}{2}(1 + T^*) - \frac{(\pi T^*)^{1/2}}{4} (3 + 2T^*) \exp(T^*) \operatorname{erfc}(T^{*1/2}) \tag{31}$$

$$b_5 = -4T^* + (\pi T^*)^{1/2} (3 + 8T^*) \exp(4T^*) \operatorname{erfc}(2T^{*1/2}) \tag{32}$$

$$b_6 = \frac{1}{2} + \frac{1}{2}(1 + 2T^*) \exp(T^*) \operatorname{erfc}(T^{*1/2}) - (T^*/\pi)^{1/2} \tag{33}$$

where erfc (x) is the usual complementary error function which was approximated using rational functions [14].

When we take the limit of $\delta \to 0$, $e \to 1$ corresponding to perfectly elastic particles, then (21)—(33) reduce to the classical results for dense hard sphere fluids ([15], [16]) and the collisional rate of energy dissipation term in (26) vanishes.

5. Simple Shear Flow

In this section, we study the case of a mean simple shear flow (constant shear rate) $\boldsymbol{u} = u(y)\, \boldsymbol{e}_x$ having no gradients of fluctuation kinetic energy or bulk density. The translational fluctuation energy equation (7) reduces to a simple balance between the shear work and the rate of dissipation

$$P_{xy} \frac{du}{dy} + \gamma = 0. \tag{34}$$

From (24), we obtain the following expressions for the shear and normal stresses

$$P_{xy} = P_{yx} = -F(\nu, T^*) \frac{5}{96} \varrho_p (\pi T)^{1/2} \sigma \frac{du}{dy} \tag{35}$$

$$P_{yy} = P_{xx} = P_{zz} = \varrho T(1 + 4b_6 \nu g_0). \tag{36}$$

Using (26), (34) and (35), we obtain a relationship for the nondimensional parameter R

$$R = \frac{\sigma\left|\frac{du}{dy}\right|}{(3T)^{1/2}} = \left[\frac{384 b_5 \nu^2 g_0}{5\pi F(\nu, T^*)}\right]^{1/2} \tag{37}$$

where

$$F(\nu, T^*) = \frac{1}{g_0 b_1}\left(1 + \frac{8}{5} b_2 \nu g_0\right)\left(1 + \frac{8}{5} b_3 \nu g_0\right) + \frac{768}{25\pi} b_4 \nu^2 g_0 . \tag{38}$$

5.1 Estimation of Mean Particle Impact Velocity

Depending upon the rate of shear, the granular particles will collide with different impact velocities. Hence, it is worthwhile to determine the range of mean impact velocities experienced by the particles in the flow system.

In a simple approximate way, we may estimate the particle's impact velocity by taking the ratio of the mean separation distance s of the particles to the mean time interval between successive collisions, i.e. $\bar{V}_i = s/\tau$. The mean particle separation distance s may be expressed in terms of (ν_m/ν) [17] as follows

$$s = \sigma[(\nu_m/\nu)^{1/3} - 1]. \tag{39}$$

The mean time between collisions τ is given by the reciprocal of the collision frequency, hence we obtain

$$\tau^{-1} = \frac{1}{n}\int_{\boldsymbol{c}_{12}\cdot\boldsymbol{k} > 0} \sigma^2(\boldsymbol{c}_{12}\cdot\boldsymbol{k})\, f^{(2)}(\boldsymbol{r} - \sigma\boldsymbol{k}, \boldsymbol{c}_1; \boldsymbol{r}, \boldsymbol{c}_2; t)\, d\boldsymbol{k}\, d\boldsymbol{c}_1\, d\boldsymbol{c}_2 . \tag{40}$$

Using (15) and (16), Eq. (40) may be evaluated readily to yield

$$\tau^{-1} = 4\pi^{1/2} n \nu^2 g_0 T^{1/2}. \tag{41}$$

Hence the mean particle impact velocity is given by

$$\bar{V}_i = \frac{24}{\pi^{1/2}} g_0[(\nu_m/\nu)^{1/3} - 1]\, T^{1/2}. \tag{42}$$

Equation (42) will be used in Section 6 to estimate $\bar{V}_i$ for the shear cell experiments of Hanes [18] and Savage and Sayed [20].

6. Comparison with Experimental Data

We may compare the theory with the experimental results for dry glass beads presented by Hanes [18], [19] and those for dry polystyrene beads obtained by Savage and Sayed [20]; both sets of data were obtained with similar annular shear

cells. In the comparisons that follow, unless otherwise specified, experimental measurements of stresses at the top plate of the annular shear cells of Savage and Sayed [20] and Hanes [18] are used. Table 1 below summarizes the materials tested in their experiments.

Table 1

Experiments	Grains	Mean dia. (mm)	Specific gravity	Max. conc.
Hanes [19]	Glass I	1.1	2.5	0.64
	Glass II	1.85	2.8	0.55
Savage and Sayed [20]	Glass III	1.80	2.97	0.552
	Polystyrene I	1.0	1.095	0.551
	Polystyrene II A	1.32	1.095	0.537
	Polystyrene II B	1.32	1.095	0.548

In the following presentations, broken curves represent calculations using the kinetic theory derived in [1] for particles with a constant coefficient of restitution whereas the solid curves represent the predictions of the present theory for particles with an e which depends upon the impact velocity. The broken curves for both the normal and shear stresses indicate a quadratic shear rate dependence in agreement with the physical arguments of Bagnold [17] for the grain inertia regime. However, most of the experimental results indicate variations with the shear rate to a power somewhat less than two. Previously, the explanation offered for the reduction in the quadratic shear rate dependence of the stresses was that it was due to the effect of dry Coulomb rubbing friction during particle overriding [20] which gives rise to shear-rate independent stress contributions. From the present results, there seems to exist another possible mechanism which can cause the stresses to vary with shear rate raised to a power of less than two. This is perhaps the major result of the present study.

By curve fitting the experimental measurements of the coefficient of restitution for glass beads as shown in Fig. 1, the dimensionless group $\delta(\varrho_p/E)^{1/2}\,|\boldsymbol{k}\cdot\boldsymbol{c}_{12}|$ is found to be about $5\times10^{-4}\,|\boldsymbol{k}\cdot\boldsymbol{c}_{12}|$. A mean value of $e=0.95$ is used in the constant e theory of [1]. Figs. 2 to 5 present some typical results of the theoretical predictions for glass beads with a mean diameter of 1.1 mm.

Fig. 2 shows the variation of the mean impact velocity of the granular particles with the shear rate for different solids fractions tested in Hanes' experiments [18]. The analysis of Section 5.1 can be used to estimate the range of impact velocities experienced by the particles. It is noted that the range of shear rates tested in the experiments was from 40 to 300 s^{-1} which corresponds to the range of mean particle impact velocities for glass beads of about 40 to 200 cm/s computed using Eq. (42). This range of impact velocities in the shear cell experiments is similar to the range of velocities tested in the coefficient of restitution experiments that are shown in Fig. 1.

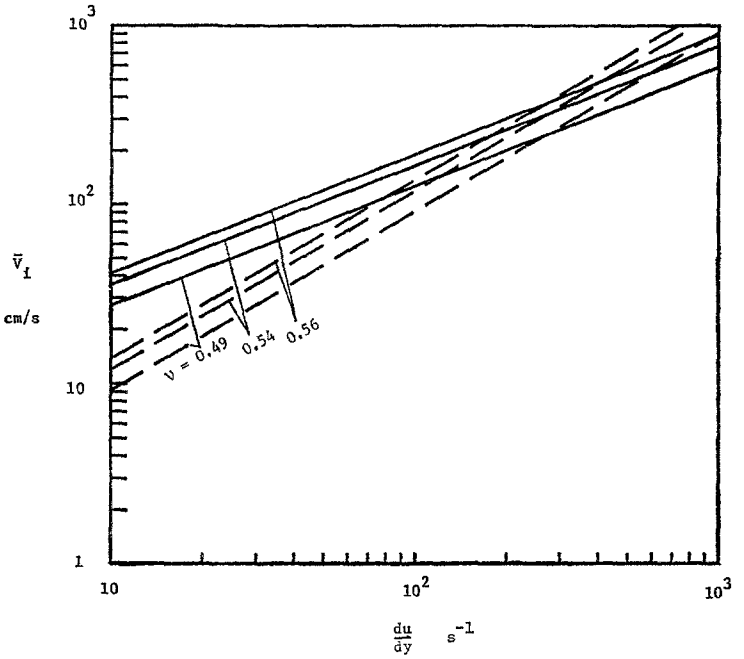

Fig. 2. Variation of mean impact velocity $\bar{V}_i$ with shear rate for the case of shearing glass beads with a mean diameter of 1.1 mm. ——, present theory; ----, constant e theory [1]

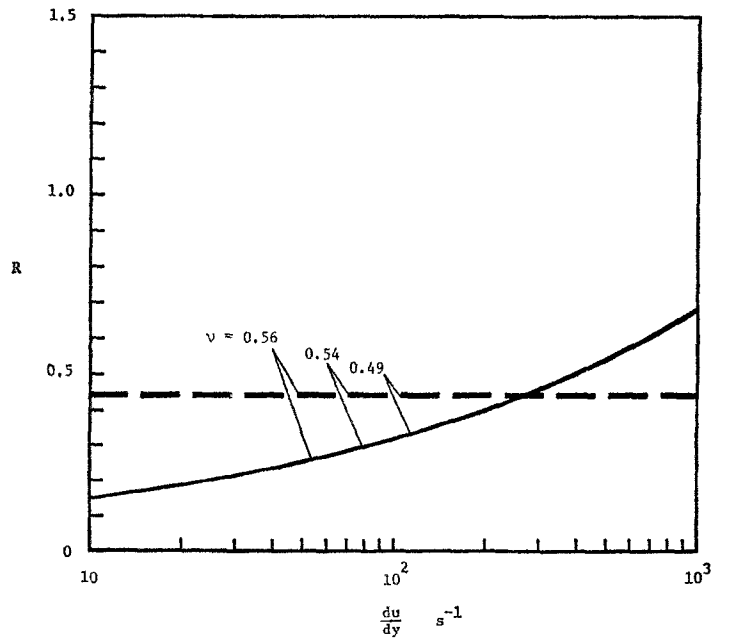

Fig. 3. Variation of R, the ratio of characteristic mean shear to r.m.s. fluctuation velocity, with shear rate for the case of shearing glass beads with a mean diameter of 1.1 mm, ——, present theory; ----, constant e theory [1]

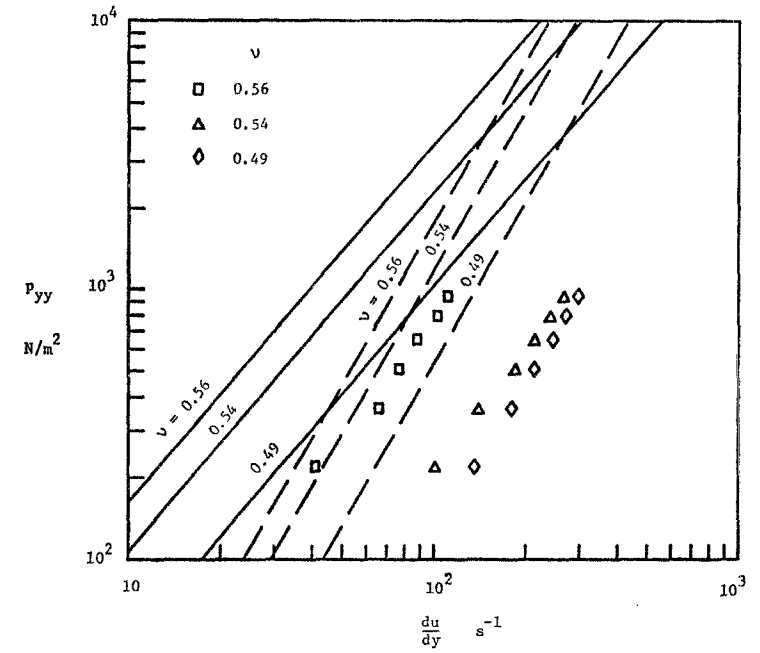
10^4
10^3
10^2
p_{yy}
N/m^2
ν
0.56
0.54
0.49
ν = 0.56
0.54
0.49
ν = 0.56
0.54
0.49
10
10^2
10^3
$\frac{du}{dy}$ s^{-1}

Fig. 4a

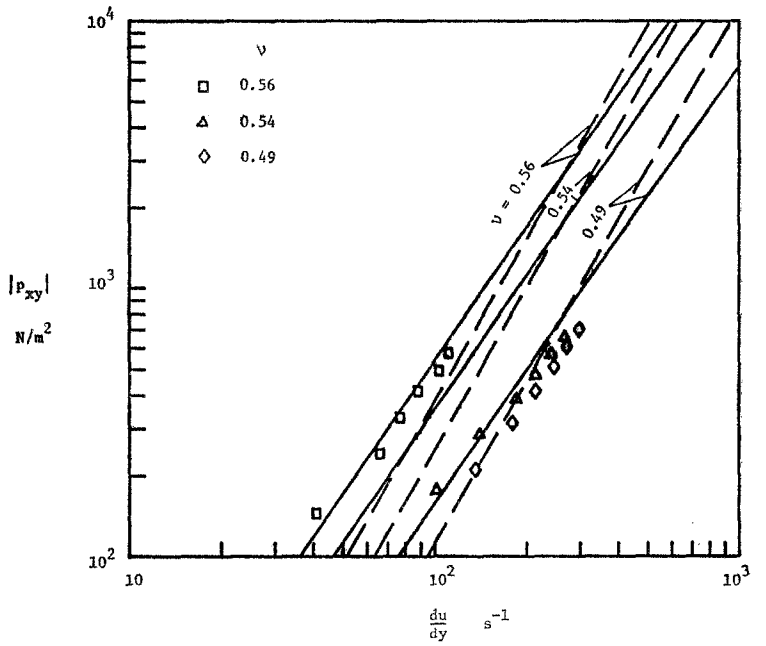
10^4
10^3
10^2
$|p_{xy}|$
N/m^2
ν
0.56
0.54
0.49
ν = 0.56
0.54
0.49
10
10^2
10^3
$\frac{du}{dy}$ s^{-1}

Fig. 4b

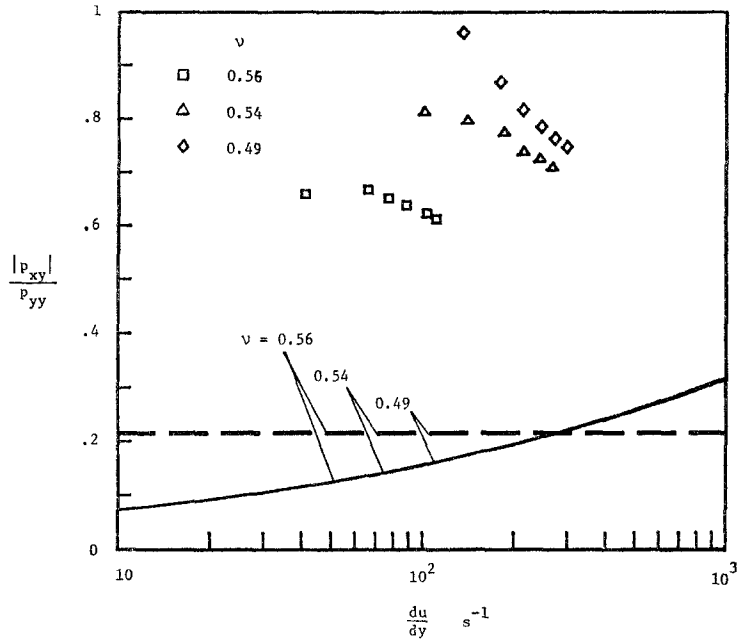

Fig. 4c

Fig. 4. Variation of *a* normal stress *b* shear stress and *c* shear to normal stress ratio with shear rate for the case of shearing glass beads with a mean diameter of 1.1 mm [18]. ——, present theory; – – –, constant e theory [1]

Fig. 3 shows the variation of the nondimensional parameter R (defined as the ratio of the mean characteristic velocity to the r.m.s. fluctuation velocity) with shear rate. The parameter R increases with increasing shear rate for the case of materials having an impact velocity dependent e whereas it is independent of shear rate for particles having a constant e.

Figs. 4.a, b, c compare the experimental results of the normal stress, the shear stress and the shear to normal stress ratio for 1.1 mm glass beads with the predictions of the two theories. The predicted normal stresses are higher than the measurements, whereas the predicted shear stresses are closer to the measured ones. Generally speaking, the predicted stresses (the solid curves) indicate variations with the shear rate raised to a power less than two which agree quite well with the experimental results. The comparisons for the stresses at solids fractions lower than 0.49 are not shown here because the experimental data were clustered together and show little dependence upon ν. At the present time, the cause for the clustering of the experimental results for solids fractions lower than 0.49 is not clear.

The predicted stress ratios are much lower than the measured values. The predicted stress ratio is independent of shear rate for materials with a constant e (broken curves) whereas the stress ratio depends on the shear rate for materials

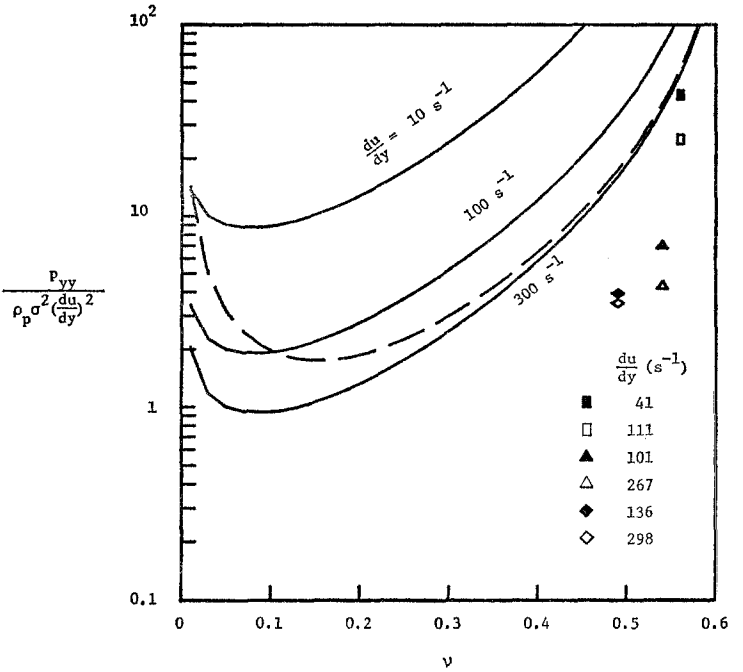
10^2
10
1
0.1
$\frac{p_{yy}}{\rho_p \sigma^2 (\frac{du}{dy})^2}$
$\frac{du}{dy}$ = 10 s^{-1}
100 s^{-1}
300 s^{-1}
$\frac{du}{dy}$ (s^{-1})
41
111
101
267
136
298
0
0.1
0.2
0.3
0.4
0.5
0.6
ν

Fig. 5a

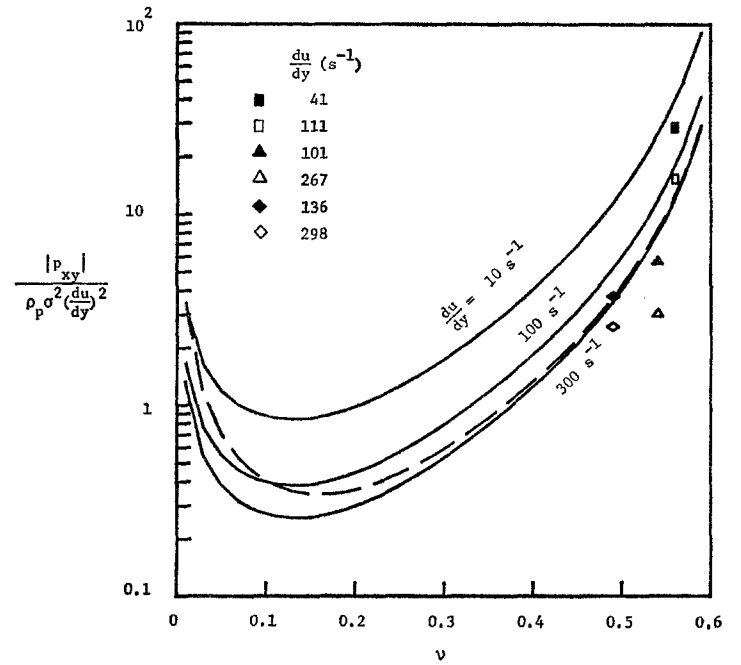
10^2
10
1
0.1
$\frac{|p_{xy}|}{\rho_p \sigma^2 (\frac{du}{dy})^2}$
$\frac{du}{dy}$ (s^{-1})
41
111
101
267
136
298
$\frac{du}{dy}$ = 10 s^{-1}
100 s^{-1}
300 s^{-1}
0
0.1
0.2
0.3
0.4
0.5
0.6
ν

Fig. 5b

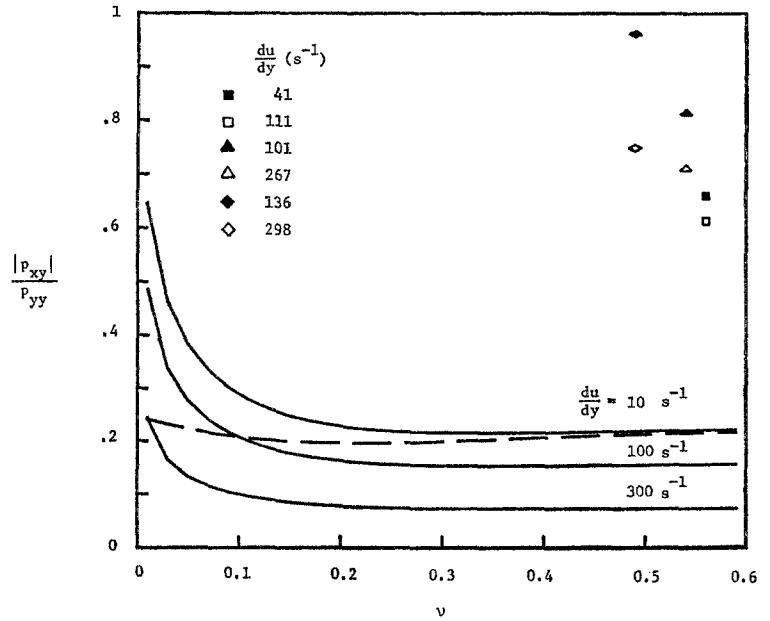

Fig. 5c

Fig. 5. Variation of non-dimensional *a* normal stress *b* shear stress and *c* shear to normal stress ratio with shear rate for the case of shearing glass beads with a mean diameter of 1.1 mm [18]. ——, present theory; - - - -, constant *e* theory [1]

with an impact velocity dependent *e* (solid curves). Both sets of calculations indicate only slight variations with concentration over the small range of solids fractions covered in the experiments. The experimental stress ratios decrease with increasing shear rate and increasing solids fraction. These trends are opposite to those suggested by the present theoretical results.

All the results in Figs. 4.a, b, c may be presented in a somewhat different manner by plotting the non-dimensional stresses versus the solids fraction for a fixed shear rate as shown in Figs. 5.a, b, c. Only the experimental measurements at the lowest and the highest shear rates for a given solids concentration tested are presented in the figures and they are denoted by solid and open symbols respectively. The present theoretical predictions show that the non-dimensional stresses decrease with increasing shear rate; this agrees qualitatively with the trend shown by the experimental results. Fig. 5a shows the variation of non-dimensional normal stress with solids fraction. One noteworthy feature of this figure is the shift of the minima when an impact velocity dependence *e* is employed instead of a constant *e*.

The quantitative discrepancies in the normal stress and the shear to normal stress ratio between the predictions of the two kinetic theories and the experimental measurements possibly are due to the incompleteness of the present analyses in which surface friction of the granular materials has been ignored.

According to the theories of [2] and [3], which incorporated the effect of particles' surface friction, the stresses were found to decrease with increasing values of the particles' surface coefficient of friction. In addition to the effect of surface friction, the kinetic theory for rough particles developed in [21] (which accounts for the effect of rotary inertia) predicts that as the surface roughness of the particles increases, the normal stress is reduced more drastically than the shear stress. As a result, the predicted stress ratio is increased. Thus, it seems possible that a proper inclusion of the effects of surface roughness and impact velocity dependent coefficient of restitution in the analysis would yield closer agreement with carefully conducted measurements.

Although the present analysis of simple shear flow has not incorporated the effect of gravity, it is interesting to compare the theoretical predictions with the measured stresses developed at different horizontal planes within the annular shear cell for shearing glass beads with mean diameter of 1.1 mm [18]. The shear stresses are assumed to be uniform in the vertical direction for the case of simple shear flow. The experimental normal stresses increase with increasing depth due to the weight of the materials being sheared. Thus, the predicted normal stresses agree somewhat better with the experimental results which are transformed to the mid-depth or the bottom of the trough of the annular shear cell. Due to lack of space these comparisons are not made here.

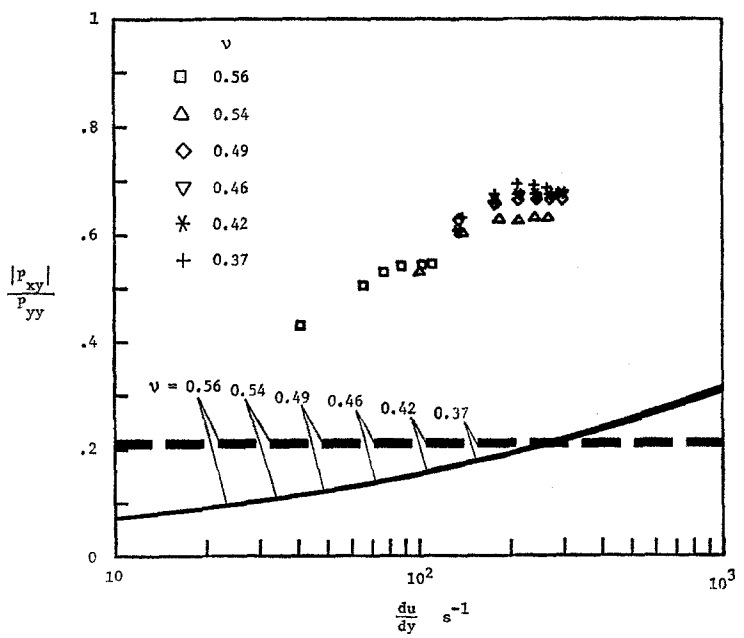

Fig. 6. Variation of shear to normal stress ratio with shear rate for the case of shearing glass beads with a mean diameter of 1.1 mm [18]. ——, present theory; ----, constant e theory [1]

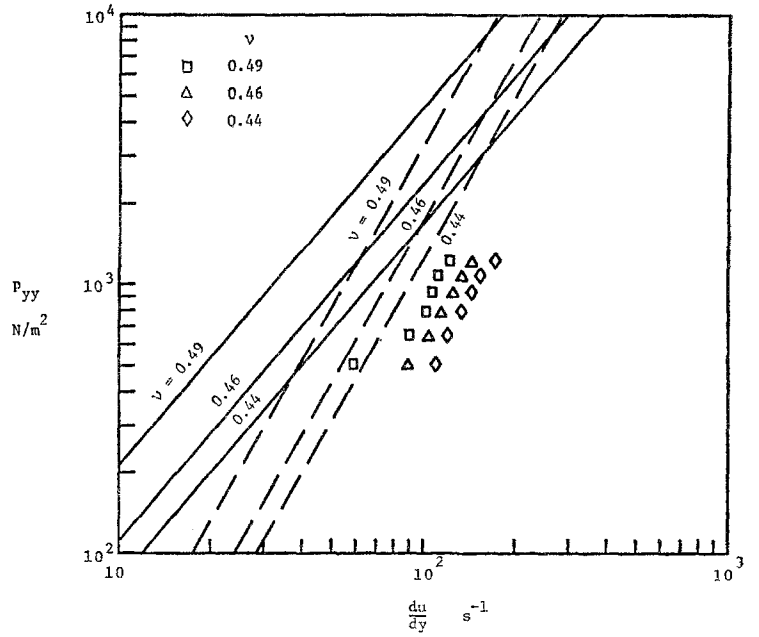
10^4
10^3
10^2
10
10^2
10^3
p_{yy}
N/m^2
$\frac{du}{dy}$ s^{-1}
ν
0.49
0.46
0.44
ν = 0.49
0.46
0.44
ν = 0.49
0.46
0.44

Fig. 7a

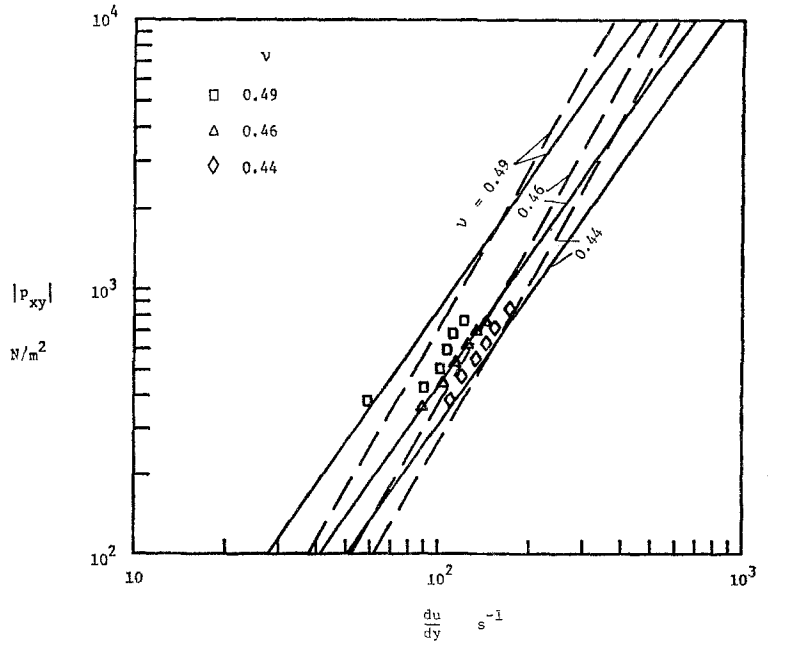
10^4
10^3
10^2
10
10^2
10^3
$|p_{xy}|$
N/m^2
$\frac{du}{dy}$ s^{-1}
ν
0.49
0.46
0.44
ν = 0.49
0.46
0.44

Fig. 7b

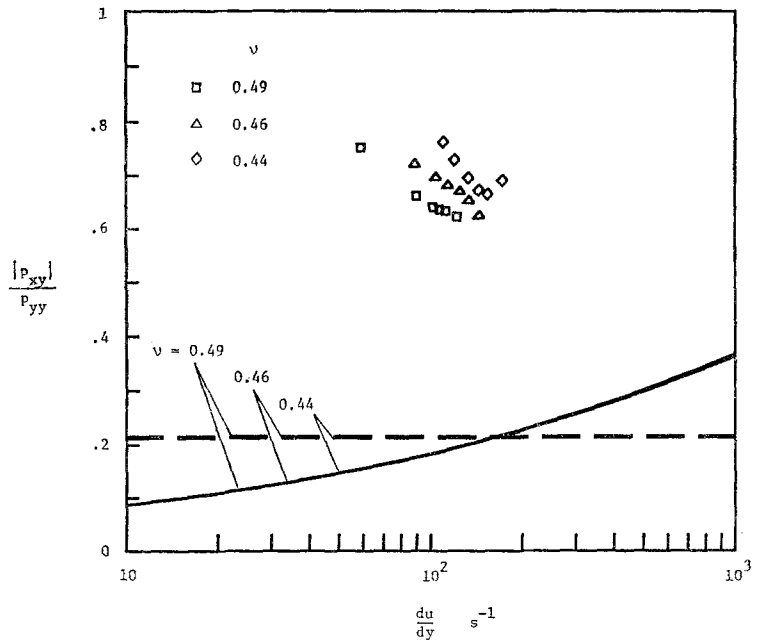

Fig. 7c

Fig. 7. Variation of *a* normal stress *b* shear stress and *c* shear to normal stress ratio with shear rate for the case of shearing glass beads with a mean diameter of 1.85 mm [18]. ——, present theory; ----, constant *e* theory [1]

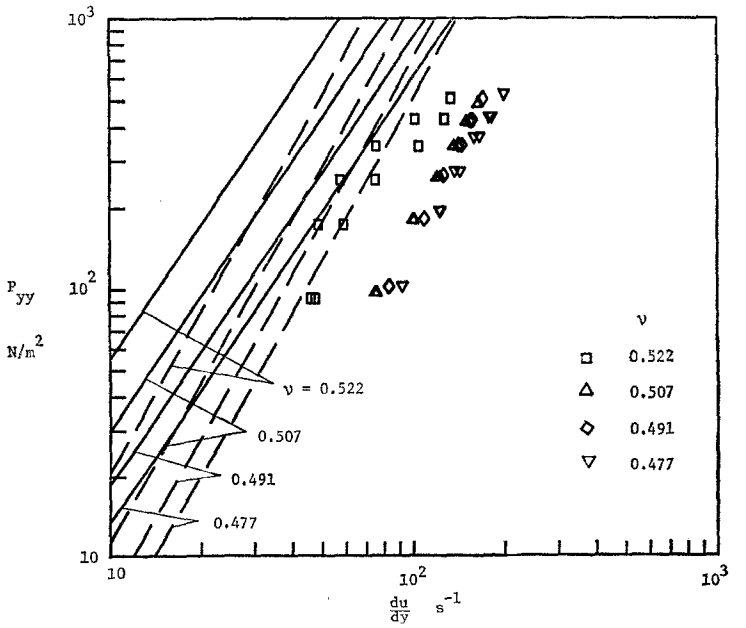

Fig. 8a

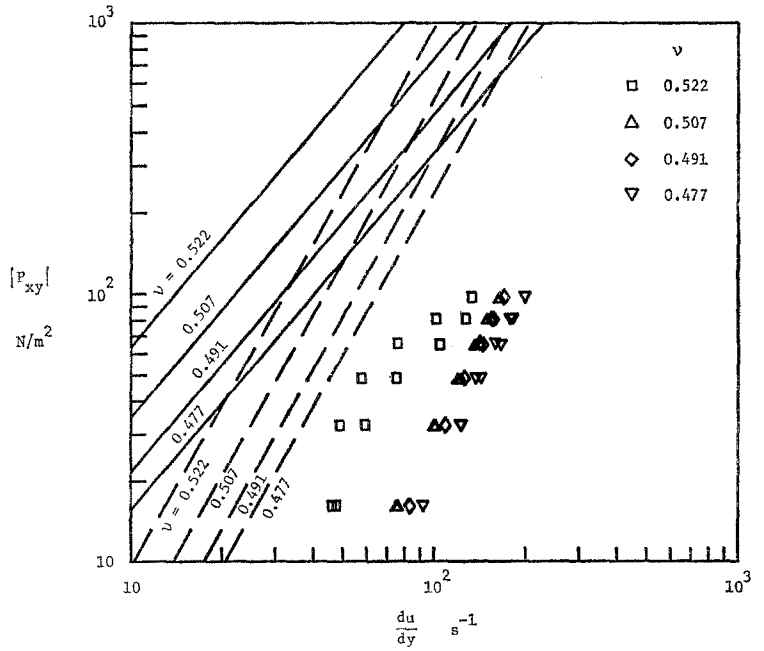

Fig. 8b

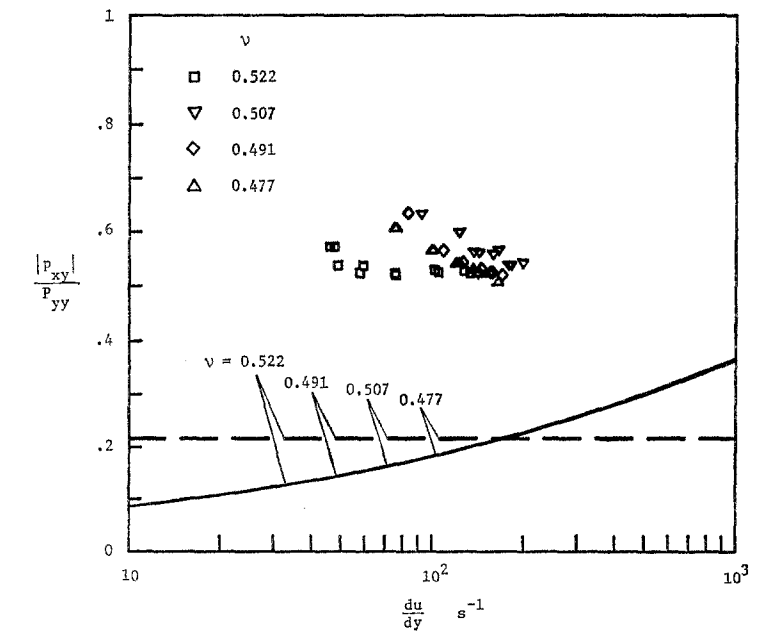

Fig. 8c

Fig. 8. Variation of *a* normal stress *b* shear stress and *c* shear to normal stress ratio with shear rate for the case of shearing glass beads with a mean diameter of 1.8 mm [20]. ——, present theory; – – –, constant *e* theory [1]

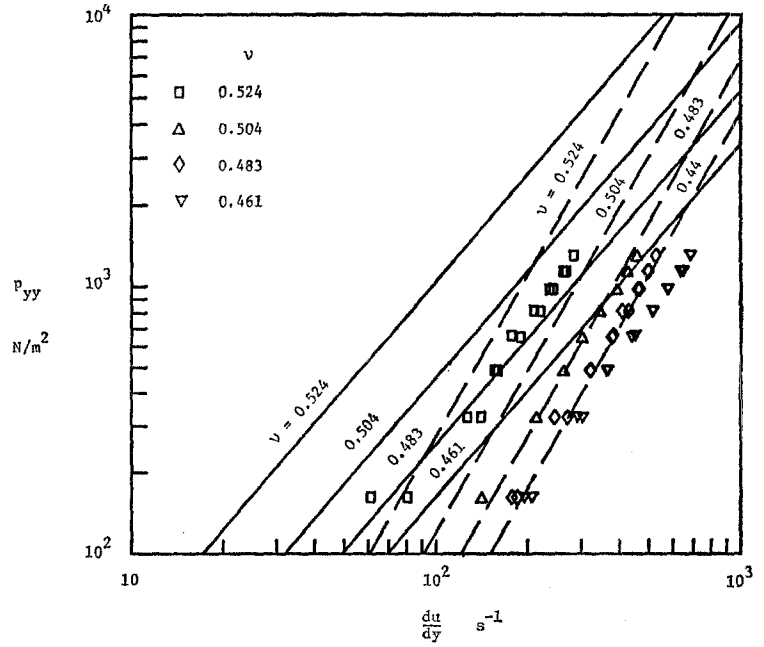
10^4
10^3
10^2
p_{yy}
N/m^2
ν
0.524
0.504
0.483
0.461
ν = 0.524
0.504
0.483
0.461
0.44
10
10^2
10^3
$\frac{du}{dy}$ s^{-1}

Fig. 9a

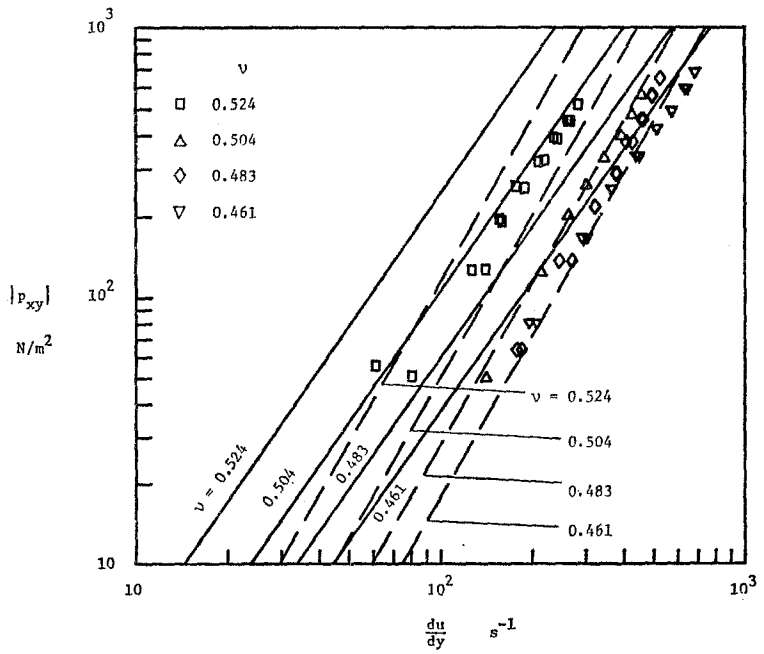
10^3
10^2
10
$|p_{xy}|$
N/m^2
ν
0.524
0.504
0.483
0.461
ν = 0.524
0.504
0.483
0.461
10
10^2
10^3
$\frac{du}{dy}$ s^{-1}

Fig. 9b

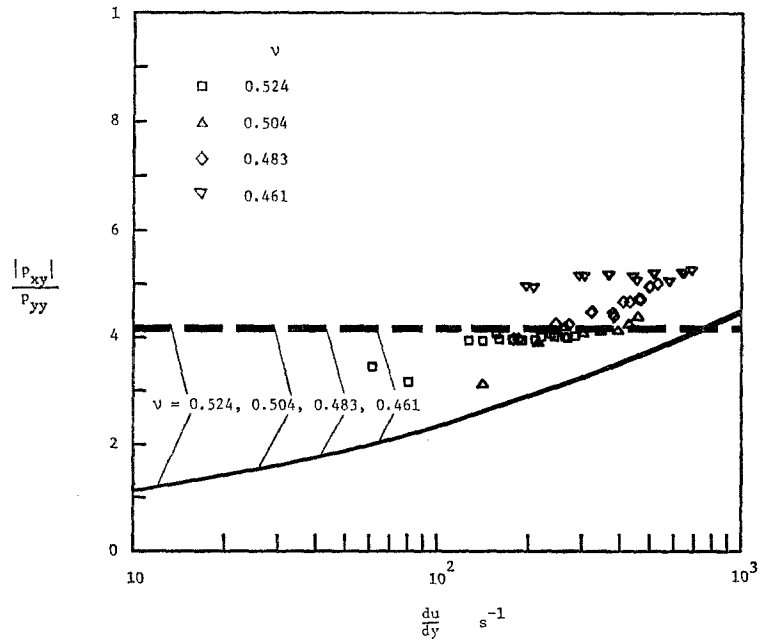

Fig. 9 c

Fig. 9. Variation of *a* normal stress *b* shear stress and *c* shear to normal stress ratio with shear rate for the case of shearing polystyrene I beads with a mean diameter of 1.0 mm [20]. ——, present theory; - - - -, constant *e* theory [1]

Only the comparisons of the predicted stress ratios with the experimental measurements transformed to the bottom of the trough are shown in Fig. 6. The agreement between the theoretical predictions and the measurements is improved when compared to that presented in Fig. 4c. The measured stress ratio increases slightly with increasing shear rate and decreasing solids fraction while the predicted stress ratio increases gradually with increasing shear rate but decreases with decreasing solids fraction. These variations of the stress ratio with shear rate and solids fraction for shearing glass beads are similar to the results obtained for shearing polystyrene beads (Figs. 9 to 11).

Figs. 7 and 8 show the comparisons of the theoretical predictions for 1.85 and 1.8 mm mean diameter glass beads with the experimental data obtained by Hanes [18] and Savage and Sayed [20] respectively. The results for the 1.85 mm glass beads are quite similar to those discussed above for the case of the 1.1 mm glass beads. However, the experimental results for the 1.8 mm glass beads are much lower than the theoretical predictions. The low values of stresses measured for the case of the 1.8 mm glass beads may have been caused by slip at the rough sand paper boundaries used in the annular shear cell of Savage and Sayed [20].

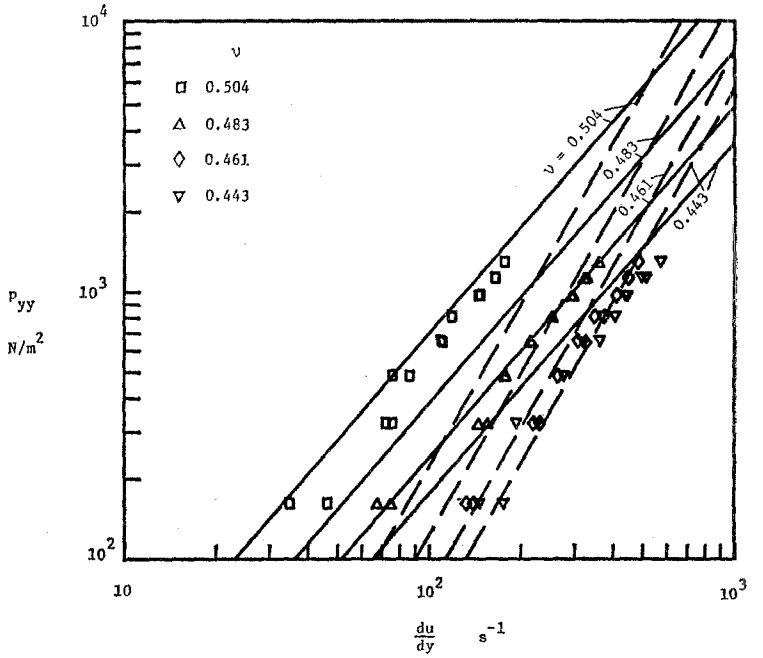

Fig. 10a

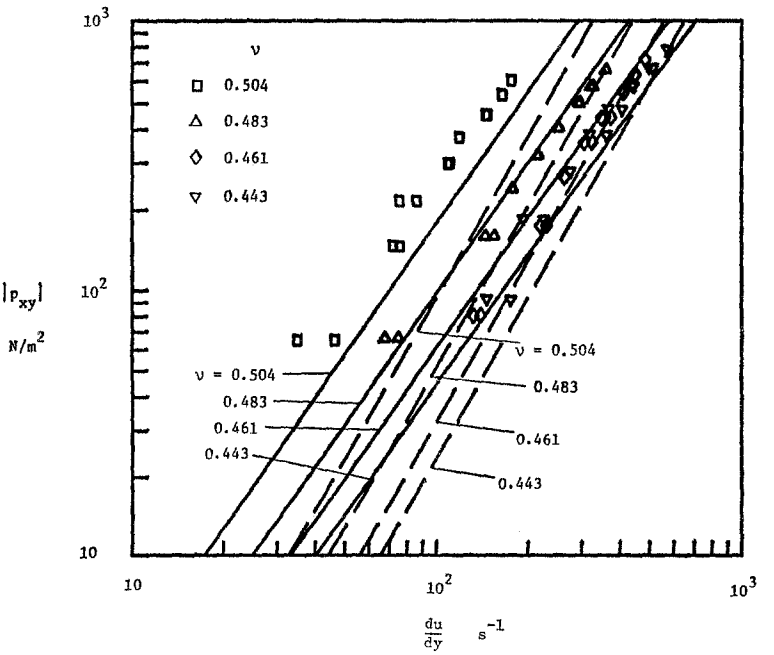

Fig. 10b

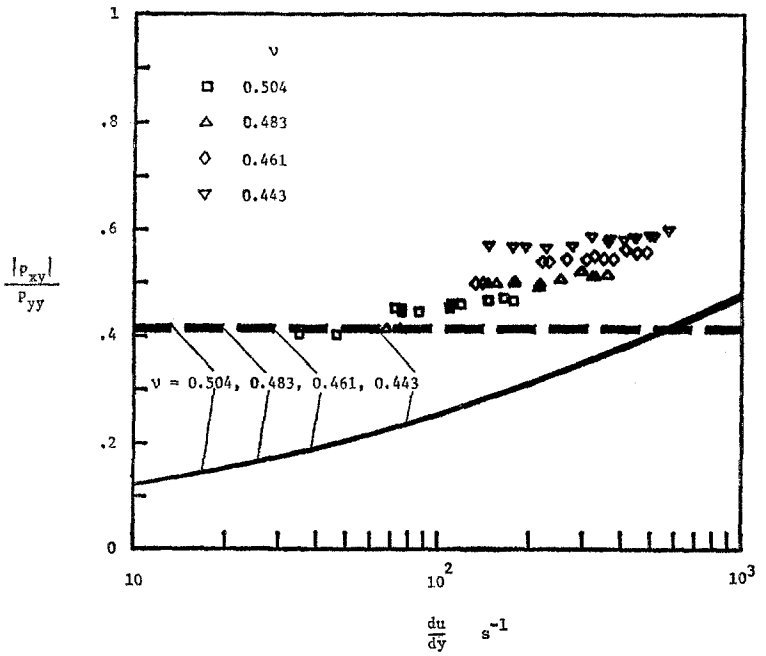

Fig. 10c

Fig. 10. Variation of *a* normal stress *b* shear stress and *c* shear to normal stress ratio with shear rate for the case of shearing polystyrene II A beads with a mean diameter of 1.32 mm [20]. ——, present theory; - - - -, constant *e* theory [1]

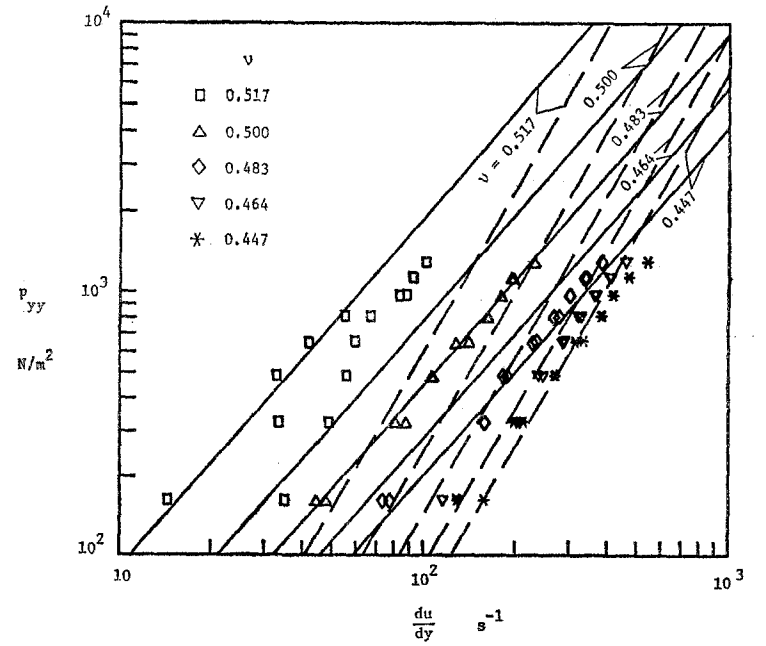

Fig. 11a

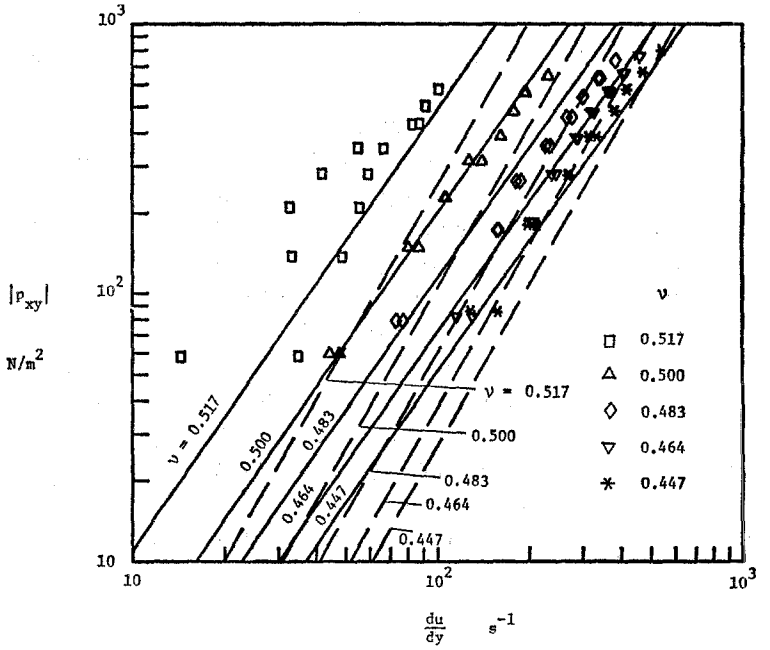

Fig. 11 b

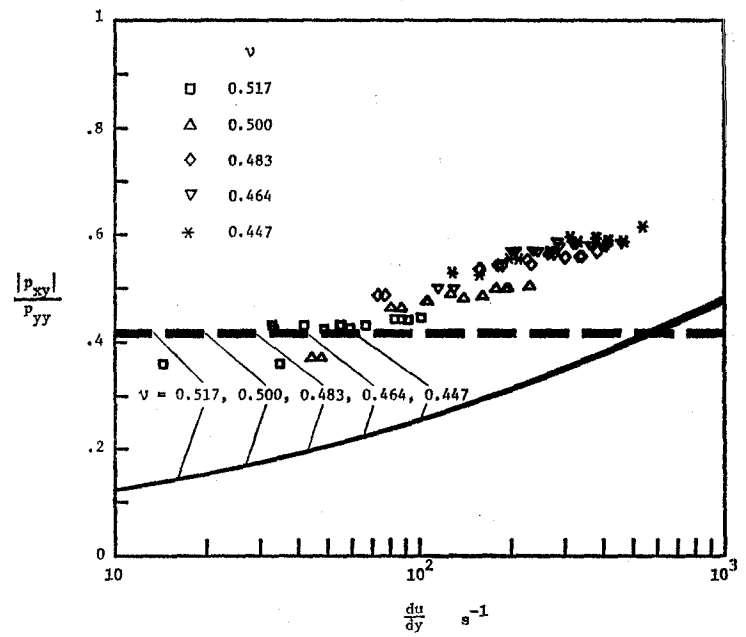

Fig. 11 c

Fig. 11. Variation of *a* normal stress *b* shear stress and *c* shear to normal stress ratio with shear rate for the case of shearing polystyrene II B beads with a mean diameter of 1.32 mm [20]. ——, present theory; - - - -, constant e theory [1]

Unfortunately, there are no experimental data available on the coefficient of restitution for the polystyrene beads as a function of impact velocity (see Appendix A). In order to make predictions of the shear cell results for sheared polystyrene particles the dimensionless group $\delta(\varrho_p/E)^{1/2}\,|\boldsymbol{k}\cdot\boldsymbol{c}_{12}|$ was assigned a value of $2\times10^{-3}\,|\boldsymbol{k}\cdot\boldsymbol{c}_{12}|$ and an e of 0.8 was used in the constant e theory of [1].

The comparisons of the theoretical predictions and the experimental results for normal and shear stresses are shown in Figs. 9 to 11. The qualitative behaviour of the stresses is similar to that for the glass beads. However, it is interesting to note that the measured stress ratios for the polystyrene beads increase slightly with increasing shear rate and decreasing solids concentration which is similar to the previous experimental results for glass beads transformed to the bottom of the trough. Since the glass beads are heavier than the polystyrene particles, gravity had a stronger effect on the normal stresses developed in sheared glass beads than those developed in the polystyrene beads. As a result, the agreement between the theoretical predictions and the experimental results measured at the top plate for the polystyrene bead tests is better than that for the glass bead tests.

7. Conclusion

The present analysis extends the kinetic theory for rapid granular flows developed in Lun, et al. [1] to consider the flow of materials having an impact velocity dependent coefficient of restitution e. An empirical exponential decay function was introduced to describe the variation of e with the impact velocity. Constitutive equations for the stress and the rate of energy dissipation were derived. The theory was then applied to the case of simple shear and the predictions were compared with the results from a number of experiments.

Experiments were performed to obtain the coefficient of restitution for glass beads. Quantitative results of e for polystyrene beads could not be obtained using the present experimental apparatus.

The predicted normal and shear stresses are proportional to the shear rate raised to a power less than two. The shear to normal stress ratio was found to increase with increasing shear rate. In addition to the effect of dry Coulomb rubbing friction as suggested by Savage and Sayed [20], the present theory shows that the effect of an impact velocity dependent e can cause the stresses to vary with the shear rate raised to a power less than two in the grain inertia regime. In general, the predicted normal stress is higher than the measurements, the predicted shear stress is in fair agreement, and hence the predicted stress ratio is low. The proper inclusion of the surface friction, rotary inertia and dry Coulomb effects in the present kinetic theory may lead to better agreement with results from carefully conducted experiments.

Appendix A: Coefficient of Restitution

A simple experiment was conducted to determine the coefficient of restitution for glass and polystyrene beads of diameter ranging from 2.0 to 2.5 mm. The test particles were fed in at the upper end of a nearly vertical glass tube and fell freely through it. At the lower end of the tube the particle bounced between two horizontal plates separated by some (adjustable) known distance H. Small electronic microphones were attached to each plate in order to pick up the signals generated by particle collisions. The signals were filtered and amplified, and were then fed into a DEC Minc-11 computer system which determined the successive real time intervals between collisions made by the particle with the top and the bottom plates. The apparatus was set up by Mr. W. Durell as a final year undergraduate project.

The simple equation of motion for a free falling spherical particle under gravity in the negative x-direction taking into account the effect of the air drag may be written as

$$\frac{du}{dt} = g - \frac{\varepsilon u^2}{\sigma} \tag{A 1}$$

where the non-dimensional parameter

$$\varepsilon = \frac{3\varrho_a C_D}{4\varrho_p}, \tag{A 2}$$

u is the particle velocity in the positive x-direction, g is the gravitational constant, ϱ_a is the density of air, C_D is the drag coefficient. An estimate of the Reynolds number in these experiments for a spherical particle of 2 mm in diameter shows that the flow is in the turbulent regime. Thus, we assume a constant drag coefficient C_D of 0.4. Since the density ratio between the air and the solid particle is small, the parameter ε is also small, i.e. $\varepsilon \ll 1$. We seek a solution for Eq. (A 1) by using a perturbation method, i.e. we expand u in terms of powers of the small parameter ε as follows

$$u = u_0 + \varepsilon u_1 + \varepsilon^2 u_2 + \cdots \tag{A 3}$$

This expansion in powers of ε is appropriate for small time and for the case in which the initial velocity is not close to the terminal velocity. Both conditions are satisfied in the present experiment. Substituting (A 3) into (A 1) and matching terms of order ε, we obtain

$$\frac{du_0}{dt} = g \tag{A 4}$$

$$\frac{du_1}{dt} = -u_0^2 \tag{A 5}$$

After integrating (A 4) and (A 5) and substituting into (A 3), we find for the first order solution

$$u = u_i + gt - (\varepsilon/\sigma)\,(u_i^2 t + u_i g t^2 + g^2 t^3/3), \tag{A 6}$$

where u_i is the initial velocity. The distance fallen is

$$x = u_i t + gt^2/2 - (\varepsilon/\sigma)\,(u_i^2 t^2/2 + u_i g t^3/3 + g^2 t^4/12). \tag{A 7}$$

Similarly, for a particle travelling vertically upward against gravity, the solutions of the velocity and the distance travelled are

$$u = u_i - gt - (\varepsilon/\sigma)\,(u_i^2 t - u_i g t^2 + g^2 t^3/3) \tag{A 8}$$

and

$$x = u_i t - gt^2/2 - (\varepsilon/\sigma)\,(u_i^2 t^2/2 - u_i g t^3/3 + g^2 t^4/12). \tag{A 9}$$

By knowing the time intervals between several successive collisions between the particle and the two plates, we may solve for the impact as well as the rebound velocities of each collision using (A 6) to (A 9) by means of iteration.

The coefficient of restitution for the glass particle colliding with fixed glass plates of 5 mm thick was obtained and its values were plotted against the impact velocity as shown in Fig. 1. The glass particles were found to bounce vigorously between the two plates. The results shown in the figure were the measurements of the first three collisions of each run.

Within the range of impact velocities tested, the range of coefficients of restitution for the glass beads were found to have values ranging from 0.97 to 0.85. These values are consistent with those presented by Goldsmith [9] from tests of colliding identical glass spheres which are many times larger in diameter than the small glass beads tested in the present experiment. For example, a typical result of $e = 0.94$ quoted by Goldsmith [9] for the glass particles was obtained by Hodgkinson [22] using two approximately identical glass spheres with diameters of about 4.12 cm. These two sets of results seem to agree with the dimensional analysis in Section 3 and the theoretical prediction of Goldsmith [9] that the coefficient of restitution is independent of particle diameter. Both sets of results show similar trends of behaviour; the coefficient of restitution e decreases slightly with increasing impact velocity.

The present results are scattered about the results presented by Goldsmith [9]. Raman [23] observed from his experiments that in order to obtain regular and consistent results for the coefficient of restitution the surfaces of the colliding balls must be clean and polished after each test. In the present experiment the beads and the plates, though they were kept clean, were never polished. This may explain in part the greater scatter of the present results. It also should be noted that the present experiments yield the coefficients of restitution between a spherical glass particle and a glass plate.

Attempts were made to determine the coefficient of restitution for the polystyrene beads, however due to various limitations in the simple experimental set up, we were unable to obtain quantitative results for e. For example, the impact waves generated by the collisions between the polystyrene bead and the plates were too weak to be sensed by the microphones.

Some qualitative tests were performed by bouncing polystyrene beads between glass plates. It was found that under the same initial conditions, the polystyrene beads bounced fewer times than the glass beads. This implies that the energy dissipated by the polystyrene bead colliding with the glass plates was probably higher than that dissipated by the glass bead. Therefore, the coefficient of restitution for the polystyrene beads would be lower than that of glass beads.

Appendix B: Radial Distribution Function

In order to evaluate the collisional integrals using the Enskog assumption for the pair velocity distribution function, we require knowledge of the radial distribution function $g_0(\nu)$. At low concentrations, the equilibrium radial distribution function which was derived from geometric considerations of collisions between hard spheres [15], [24] may be written as

$$g_0(\nu) = 1 + 2.5\nu + 4.592\nu^2 + 7.36\nu^3. \tag{B 1}$$

In [1], we have used the empirical formula for $g_0(\nu)$ due to Carnahan and Starling [25]

$$g_0(\nu) = \frac{2 - \nu}{2(1 - \nu)^3} \tag{B 2}$$

which agrees with molecular dynamics calculations up to $\nu = 0.5$.

Savage [26] has suggested that the expression given by Ogawa et al. [2]

$$g_0(\nu) = [1 - (\nu/\nu_m)^{1/3}]^{-1} \tag{B 3}$$

may be more appropriate for use in the expression for $f^{(2)}$ at high concentrations during shearing than Eq. (B 2). However, at low concentrations Eq. (B 3) is not consistent with Eq. (B 1) and does not agree with the molecular dynamics calculations.

We propose another expression for the radial distribution function

$$g_0(\nu) = (1 - \nu/\nu_m)^{-5\nu_m/2} \tag{B 4}$$

which may be more appropriate for use at high concentrations during *shearing* for small finite systems than Eqs. (B 1) to (B 3). When Eq. (B 4) is expanded in power series for small ν, the first two terms are same as those derived in (B 1).

Eqs. (B 1) to (B 4) were plotted in Fig. 12 together with the results from the

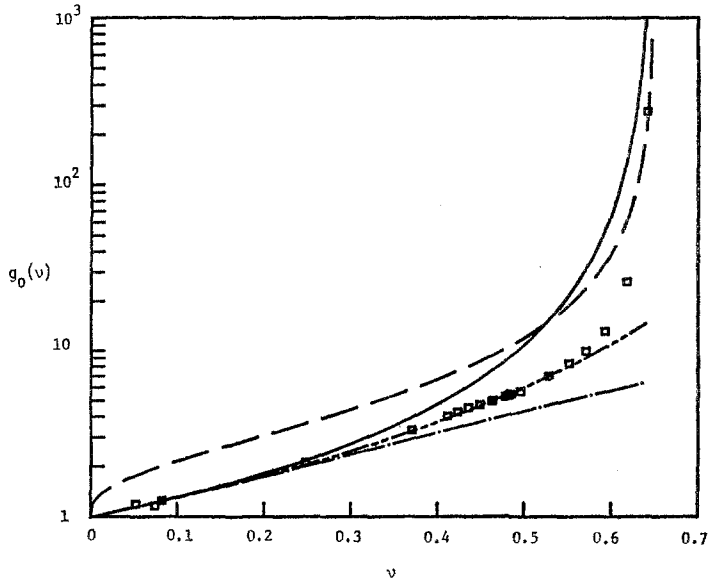

Fig. 12. Variation of radial distribution function with solids fraction. □, molecular dynamics computations [27]; —·—, [15]; —··—, [25]; ----, [2]; ——, present theory

molecular dynamics calculations [27]. The computer simulations were performed up to a volume concentration of about 0.641 under *equilibrium* conditions and with the use of periodic boundaries. The computation yielded a large increase in the normal stress and consequently a large increase in $g_0(\nu)$ (see for example Eq. (36)) at concentrations near the maximum concentration ν_m for random closest packing of the system.

The radial distribution function proposed in (B 4) accounts for the drastic increase in $g_0(\nu)$ as ν approachs ν_m. In order for the equilibrium radial distribution function of Carnahan and Starling (B 2) to describe the same increase in $g_0(\nu)$, ν has to increase to unity which is physically impossible for identical hard spheres. For finite granular systems, the value of ν_m can be as low as 0.55 or so depending upon the size and geometry of the shear space in the test devices [17], [19]. We repeat, the present form of Eq. (B 4) is proposed for shearing motion whereas that of Carnahan and Starling (B 2) was based upon simulations involving no mean motion.

Acknowledgement

Grateful acknowledgement is made to the National Sciences and Engineering Research Council of Canada (NSERC) for support of this work through an NSERC operating grant. C. K. K. Lun was supported by an NSERC Postgraduate Scholarship. The authors are indebted to C. S. Campbell and D. M. Hanes for useful discussions and comments regarding a first draft of this paper.

References

[1] Lun, C. K. K., Savage, S. B., Jeffrey, D. J., Chepurniy, N.: Kinetic theories for granular flow: inelastic particles in Couette flow and slightly inelastic particles in general flow field. J. Fluid Mech. **140**, 223–256 (1984).

[2] Ogawa, S., Umemura, A., Oshima, N.: On the equations of fully fluidized granular materials. Z. angew. Math. Phys. **31**, 483–493 (1980).

[3] Shen, H. H., Ackermann, N. L.: Constitutive relationships for fluid-solid mixtures. J. Eng. Mech. Div. ASCE **108**, 748–763 (1982).

[4] Haff, P. K.: Grain flow as a fluid-mechanical phenomenon. J. Fluid Mech. **134**, 401–430 (1983).

[5] Jenkins, J. T., Savage, S. B.: A theory for the rapid flow of identical, smooth, nearly elastic particles. J. Fluid Mech. **130**, 187–202 (1983).

[6] Campbell, C. S., Brennen, C. E.: Computer simulation of shear flows of granular material, in: Mechanics of granular materials: New constitutive relations (Jenkins, J. T., Satake, M., eds.), pp. 313–326. Elsevier 1983.

[7] Shen, H. H., Ackermann, N. L.: Constitutive equations for simple shear flow of a disk shaped granular mixture. Int. J. Eng. Science **22** (7), 829–843 (1984).

[8] Walton, O. R., Braun, R. L.: Viscosity, granular-temperature and stress calculations for shearing assemblies of inelastic, frictional disks. Presented at the 56th Annual Meeting of the Society of Rheology, Feb. 1985. J. of Rheology (Submitted).

[9] Goldsmith, W.: Impact: The theory and physical behavior of colliding solids. Arnold 1960.

[10] Trulsen, J.: Towards a theory of jet streams. Astrophys. Space Sci. **12**, 329–348 (1971).

[11] Hameen-Anttila, K. A.: An improved and generalized theory for the collisional evolution of Keplerian systems. Astrophys. Space Sci. **58**, 477–519 (1978).

[12] Goldreich, P., Tremaine, S.: The velocity dispersion in Saturn's rings. ICARUS **34**, 227–239 (1978).

[13] Stewart, G. R., Lin, D. N. C., Bodenheimer, P.: Collision-induced transport processes in planetary rings, in: Planetary rings (Greenberg, R., Brahic, A., eds.). University of Arizona Press 1984.

[14] Abramowitz, M., Stegun, I. A.: Handbook of mathematical functions. Appl. Math. Ser. **55**, 1965.

[15] Chapman, S., Cowling, T. G.: The mathematical theory of non-uniform gases, 3rd edn. Cambridge University Press 1970.

[16] Davis, H. T.: Kinetic theory of dense fluids and liquids revisited. Adv. Chem. Phys. **24**, 257–343 (1973).

[17] Bagnold, R. A.: Experiments on a gravity free dispersion of large solid spheres in a Newtonian fluid under shear. Proc. Roy. Soc. **A 225**, 49–63 (1954).

[18] Hanes, D. M.: Studies on the mechanics of rapidly flowing granular-fluid materials. Ph.D. dissertation, University of California 1983.

[19] Hanes, D. M., Inman, D. L.: Observations of rapidly flowing granular-fluid materials. J. Fluid Mech. **150**, 357–380 (1985).

[20] Savage, S. B., Sayed, M.: Stresses developed by dry cohesionless granular materials sheared in an annular shear cell. J. Fluid Mech. **142**, 391–430 (1984).

[21] Lun, C. K. K., Savage, S. B.: A simple kinetic theory for granular flow of rough, inelastic, spherical particles. J. Appl. Mech. (1985) (Submitted).

[22] Hodgkinson, E.: On the imperfectly elastic bodies. Transactions of the British Association of Science **4**, 534–543 (1834).

[23] Raman, C. V.: The photographic study of impact at minimal velocities. Physical Review **12** (6), 442—447 (1918).
[24] Hirschfelder, J. O., Curtis, C. R., Bird, R. B.: The molecular theory of gases and liquid. New York: Wiley 1954.
[25] Carnahan, N. F., Starling, K. E.: Equations of state for non-attracting rigid spheres. J. Chem. Phys. **51**, 635—636 (1969).
[26] Savage, S. B.: Streaming motions in a bed of vibrationally-fluidized dry granular material. J. Fluid Mech. (1986) (Submitted).
[27] Alder, B. J., Wainwright, T. E.: Studies in molecular dynamics. II. Behavior of a small number of elastic spheres. J. Chem. Phys. **33** (5), 1439—1451 (1960).

Dr. C. K. K. Lun and Prof. S. B. Savage
Department of Civil Engineering and Applied Mechanics
McGill University
817 Sherbrooke Street West
Montreal, PQ
Canada H3A 2K6